Hindawi Publishing Corporation
Journal of Nanotechnology
Volume 2015, Article ID 172864, 10 pages
http://dx.doi.org/10.1155/2015/172864

*Research Article*

# Optical and Sensing Properties of Cu Doped ZnO Nanocrystalline Thin Films

**R. K. Shukla,[1] Anchal Srivastava,[1] Nishant Kumar,[1] Akhilesh Pandey,[2] and Mamta Pandey[1]**

[1]*Department of Physics, University of Lucknow, Lucknow 226007, India*
[2]*Solid State Physics Laboratory (SSPL), DRDO, New Delhi 110054, India*

Correspondence should be addressed to Anchal Srivastava; asrivastava.lu@gmail.com

Received 22 July 2015; Accepted 29 September 2015

Academic Editor: Wen Zeng

Copyright © 2015 R. K. Shukla et al. This is an open access article distributed under the Creative Commons Attribution License, which permits unrestricted use, distribution, and reproduction in any medium, provided the original work is properly cited.

Undoped and Cu doped ZnO films of two different molarities deposited by spray pyrolysis using zinc nitrate and cupric chloride as precursors show polycrystalline nature and hexagonal wurtzite structure of ZnO. The crystallite size varies between 10 and 21 nm. Doping increases the transmittance of the films whereas the optical band gap of ZnO is reduced from 3.28 to 3.18 eV. With increment in doping the surface morphology changes from irregular shaped grains to netted structure with holes and then to net making needle-like structures which lends gas sensing characteristics to the films. Undoped ZnO shows maximum sensitivity at 400°C for higher concentration of $CO_2$. The sensitivity of Cu doped sample is maximum at 200°C for all $CO_2$ concentrations from 500 to 4000 ppm.

## 1. Introduction

Zinc oxide, an environmentally safe and economic material, with wide direct band gap (3.37 eV) and large exciton binding energy (60 meV) at room temperature [1–3] finds application in fabrication of various devices including ultraviolet (UV) light-emitters, varistors, transparent high power electronics, piezoelectric transducers, gas sensors, smart windows, and solar cells [4–6]. It is one of the most important II-VI compound semiconductors and its application in optoelectronics can be expanded by altering its band gap energy. Doping of any metal can alter the band gap and/or can introduce energy levels in the band gap of semiconductor materials [7, 8]. Some metals can assume a valency depending on their chemical surrounding, for example, any copper salt when doped in ZnO using organometallic solution can lead to varied oxidation states of Cu [9]. The film based gas sensors depending on the detection of variation in some electrical parameter, resistance or capacitance, of the film utilize n-type semiconducting metal oxides such as ZnO. Also, metal oxides are stable at elevated temperatures in air [10].

There are several methods for producing ZnO based films, for example, chemical vapor deposition, thermal evaporation, magnetron sputtering, pulsed laser deposition (PLD), laser chemical vapor deposition, and nonvacuum methods, namely, successive ionic layer absorption and reaction (SILAR), sol-gel spin coating, spray pyrolysis, screen printing, and so forth [1, 7, 11–18]. Wet chemical techniques offer easy way for homogeneous doping of virtually any element in any proportion by merely adding it in some form of cationic solution. Moreover, these techniques do not require high quality targets and/or substrates which are unavoidable in sputtering and PLD. SILAR does not involve high temperatures allowing employment of polymers as substrates. Besides, sol-gel spin coating is a time saving process; however, it is difficult to precisely control the thickness of the films. In spray pyrolysis, oxides can be readily obtained by thermal decomposition of organometallic precursor solution during its spraying on adequately heated substrate responsible for good quality films. Thickness of the film as well as the deposition rate can be controlled over a wide range by changing the spray parameters. Also large area deposition can be done using this method. Local overheating leading to degradation of film does not occur here which is generally a matter of concern in radio frequency magnetron sputtering due to involvement of high power sources [19].

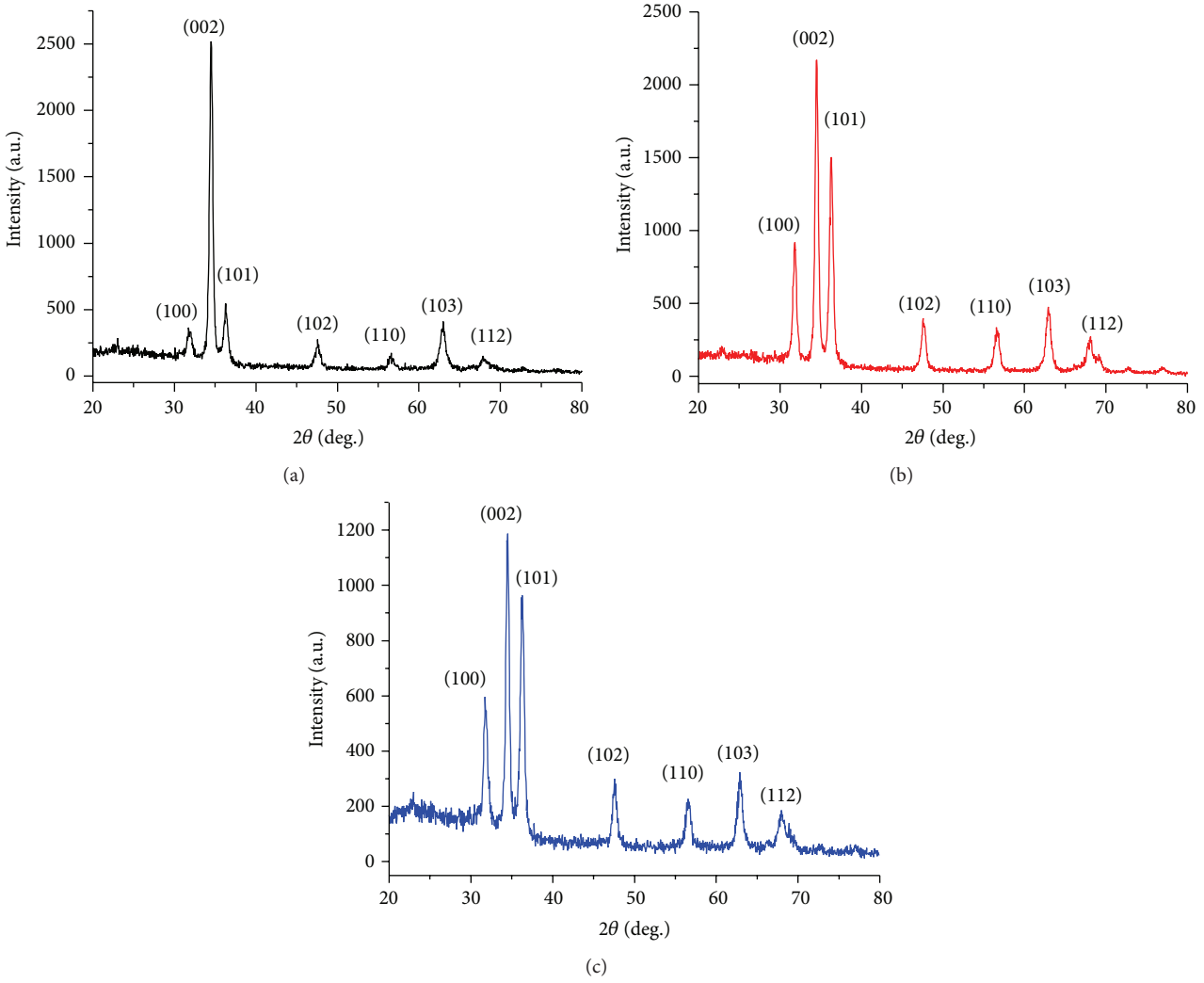


Figure 1: XRD pattern of undoped and Cu doped ZnO thin films sample. Here (a), (b), and (c) correspond to samples Z1, Z1C1, and Z1C2, respectively, prepared using precursor solution of molarity of 0.1 M.

In this paper, structural, optical, and morphological property of undoped and Cu doped ZnO thin films prepared by spray pyrolysis along with $CO_2$ sensing [20] has been presented.

## 2. Experimental

The precursor for undoped films is prepared by obtaining 0.1 and 0.15 M solutions of zinc nitrate (99.9% pure, S D Fine Chem. Ltd.) in deionized water. The mixture is magnetically stirred at 60°C for 30 min to get homogeneous solution. To this solution, appropriate volumes of 0.1 and 0.15 M solutions of cupric chloride in deionized water are added to obtain 1 and 2 at.% doping of Cu. These solutions are again stirred for 30 min. Both the undoped and doped solutions are aged for 15 days for obtaining stability.

The experimental set-up contains glass atomizer for spraying the precursor solution. The substrates are kept on hot iron plate which is attached with thermocouple and temperature controller to maintain the required temperature. The precursor solution is introduced in the container connected to the liquid inlet of the atomizer by a tube having solution flow controller and the compressed air used as carrier gas is let into the gas inlet of the atomizer [17].

For deposition of thin film, 10 mL of the precursor solution of each sample, one at a time, is transferred to the container. The distance between nozzle and the substrate is set at 25 cm and the flow rate is set at at 10 mL/min. The substrate temperature was maintained at 400°C to obtain good quality films in addition to thermal decomposition of zinc nitrate. Reactions occurring during deposition are as follows:

$$\begin{aligned} &Zn(NO_3)_2 \cdot 6H_2O + H_2O \longrightarrow Zn(OH)_2 + 2NO_2\uparrow + 7H_2O\uparrow \\ &Zn(OH)_2 \longrightarrow ZnO + H_2O\uparrow \end{aligned} \quad (1)$$

Postdeposition annealing of the films is done at 400°C for 30 minutes. These six samples, undoped ZnO, ZnO: 1 at.%

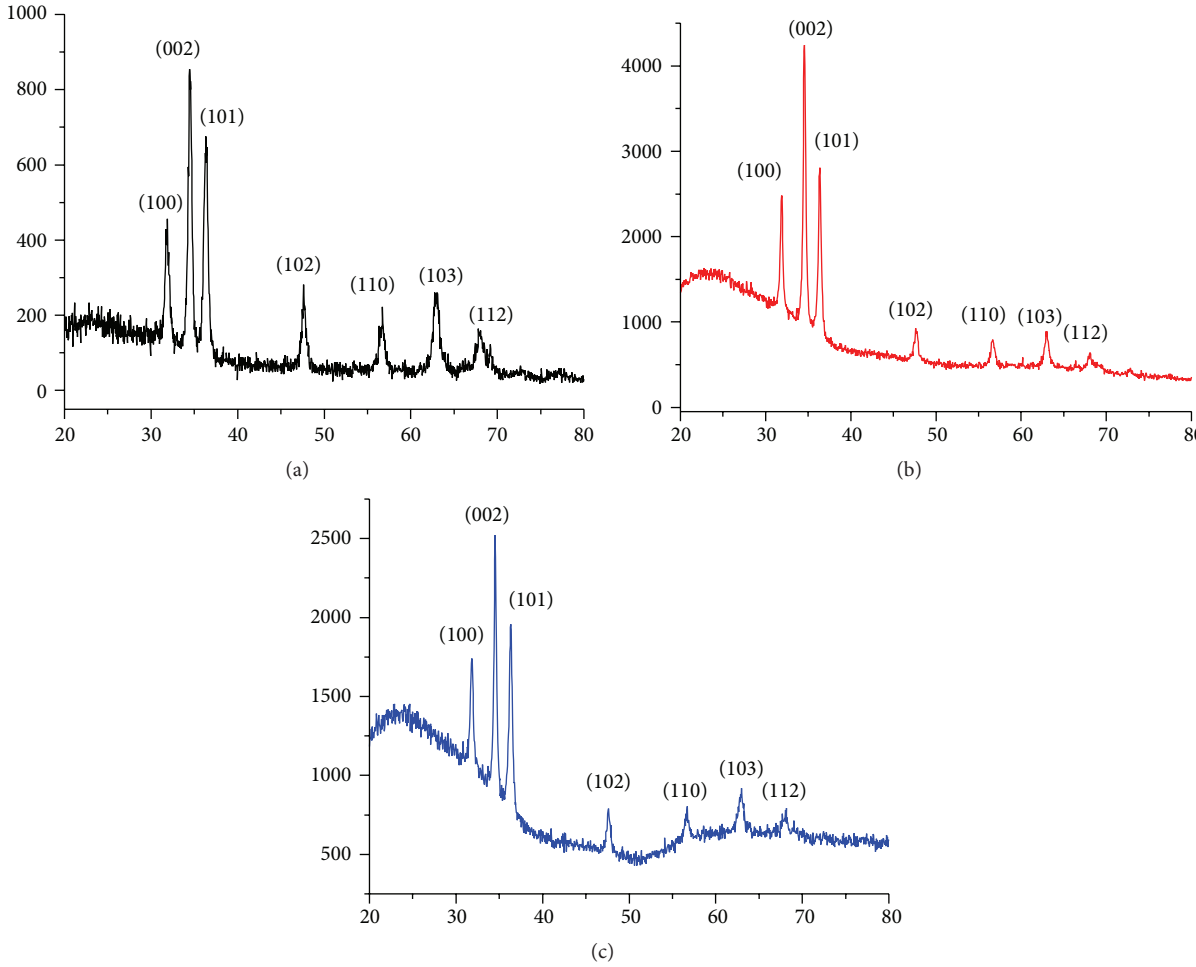


FIGURE 2: XRD pattern of undoped and Cu doped ZnO thin films sample. Here (a), (b), and (c) correspond to samples Z2, Z2C1, and Z2C2, respectively, prepared using precursor solution of molarity of 0.15 M.

Cu and ZnO: 2 at.% Cu using 0.1 M and 0.15 M precursor solutions, are named as Z1, Z1C1, and Z1C2 and Z2, Z2C1, and Z2C2, respectively. Deposition parameters have been strictly kept the same to obtain films of approximately similar thickness.

The crystal phase and crystallinity of the samples have been investigated using X-ray diffractometer (Bruker D8 Advance X-ray diffractometer) for $2\theta$ values ranging from 20 to 80° using CuK$\alpha$ radiation ($\lambda$ = 0.154 nm). Transmittance spectra have been recorded using UV-Vis spectrophotometer (model number 108 Make-Systronics). Surface morphology is obtained using FESEM (ZEISS) and film thickness is determined by XP-1 stylus profiler (Ambios Technology).

## 3. Characterization

*3.1. X-Ray Diffraction.* The X-ray diffraction patterns for samples Z1, Z1C1, and Z1C2 are shown in Figure 1 and for samples Z2, Z2C1, and Z2C2 are shown in Figure 2. All the samples exhibit hexagonal wurtzite structure of ZnO showing preferred orientations along (100), (002), and (101) [1, 15, 21–23]. The peak along $c$-axis, that is, (002) plane, occurs at $2\theta$ = 34.50, 34.54°, and 34.47° for samples Z1, Z1C1, and Z1C2, respectively. The diffraction peak shifts to higher value for Z1C1 and back to lower value of $2\theta$ for sample Z1C2. This indicates that initially Cu substitutes Zn and with increasing concentration of Cu it goes into interstitial position. For samples Z2, Z2C1, and Z2C2, $2\theta$ = 34.46°, 34.50°, and 34.50°, respectively. The diffraction peak shifts to higher value as dopant is introduced and remains unaffected thereafter. Diffraction peak except those for ZnO is not found for any of the samples, indicating absence of any impurity phase. Crystallite size along (002) crystallographic plane for these samples, as calculated by Debye Scherer formula, lies between 10 and 21 nm, Table 1. The orientation parameter $\gamma_{(hkl)} = (I_{(hkl)}/\sum(I_{(hkl)}))$ [1], Table 1, varies from 0.127 to 0.772 indicating dominant orientation along (002) plane.

*3.2. UV-Visible Spectra and Optical Band Gap.* The transmittance spectra of samples prepared using precursor solutions of molarities 0.1 M and 0.15 M are shown in Figures 3 and 4, respectively. The transmittance of samples Z1, Z1C1, and

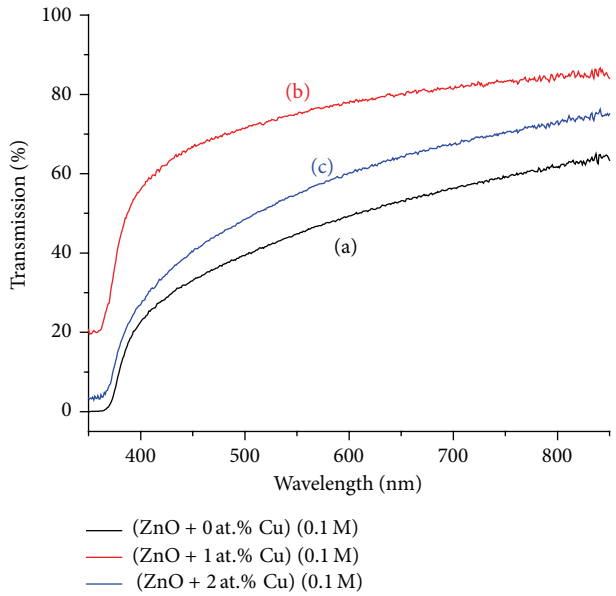


Figure 3: Transmission spectra of undoped and Cu doped ZnO thin films sample. Here (a), (b), and (c) correspond to samples Z1, Z1C1, and Z1C2, respectively, prepared using precursor solution of molarity of 0.1 M.

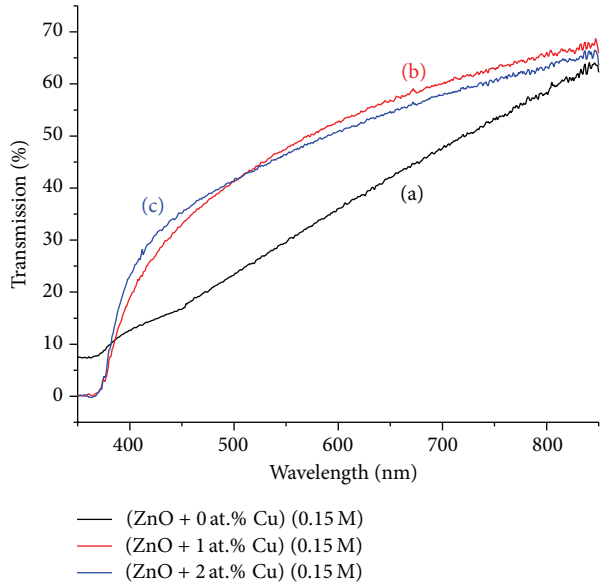


Figure 4: Transmission spectra of undoped and Cu doped ZnO thin films sample. Here (a), (b), and (c) correspond to samples Z2, Z2C1, and Z2C2, respectively, prepared using precursor solution of molarity of 0.15 M.

Z1C2 increases gradually up to 87% over the range of 350 to 850 nm, Figure 3. The maximum transmittance for samples Z2, Z2C1, and Z2C2 is nearly 69% at 847 nm. Undoped film of lower molarity is more transparent at optical wavelengths, whereas around 800 nm both of the undoped films have similar transmittance. High transmittance indicates that the obtained films are of low impurities and have only few lattice defects [24]. Doped films are comparatively more transparent. In general, the transmittance is found to decrease with an increase in molarity of the precursor solution as expected. The decrease in transmittance may be due to free carrier absorption of photons [25].

The thickness of 0.1 M samples Z1, Z1C1, and Z1C2 is 1080, 1100, and 1050 nm, respectively. For 0.15 M samples Z2, Z2C1, and Z2C2, the thickness is 1120, 1090, and 1100 nm, respectively. The optical band gap of the films determined by Tauc's plot is found to vary over a range of 3.18 to 3.28 eV, Table 2. The variation in

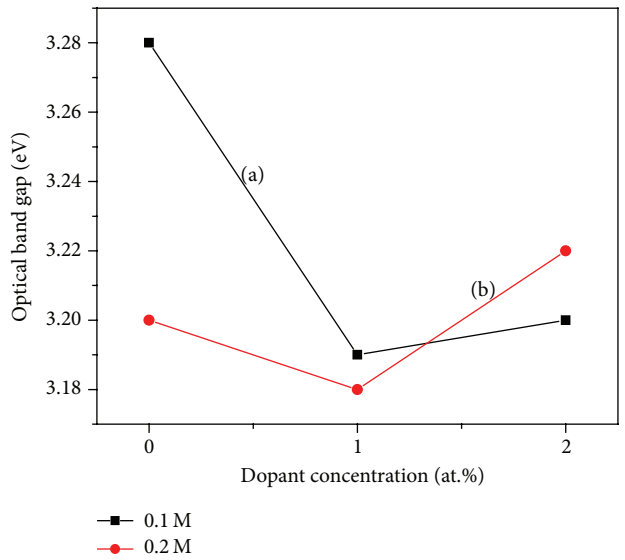


Figure 5: The variation in band gap (a) and (b) corresponds to the sample prepared using precursor solution of molarity of 0.1 and 0.15 M, respectively.

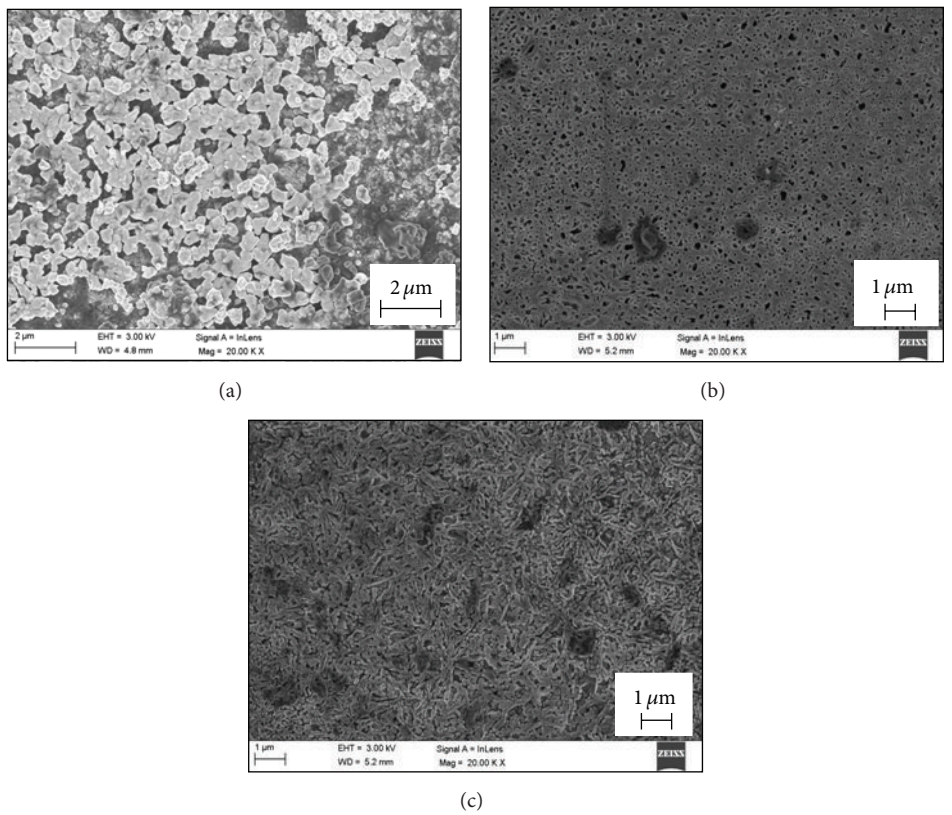


Figure 6: SEM of undoped and Cu doped ZnO thin films prepared using precursor solution of molarity of 0.1 M. Here (a), (b), and (c) correspond to samples Z1, Z1C1, and Z1C2, respectively.

band gap due to doping and molar concentration is shown in Figure 5. For undoped ZnO, the band gap decreases with increase in molarity of the precursor solution.

*3.3. Surface Morphology.* The scanning electron micrographs (SEM) for the three samples corresponding to 0.1 M molarity are shown in Figure 6. Sample Z1, that is, undoped ZnO of molarity 0.1 M, has flakes-like structures connected to each

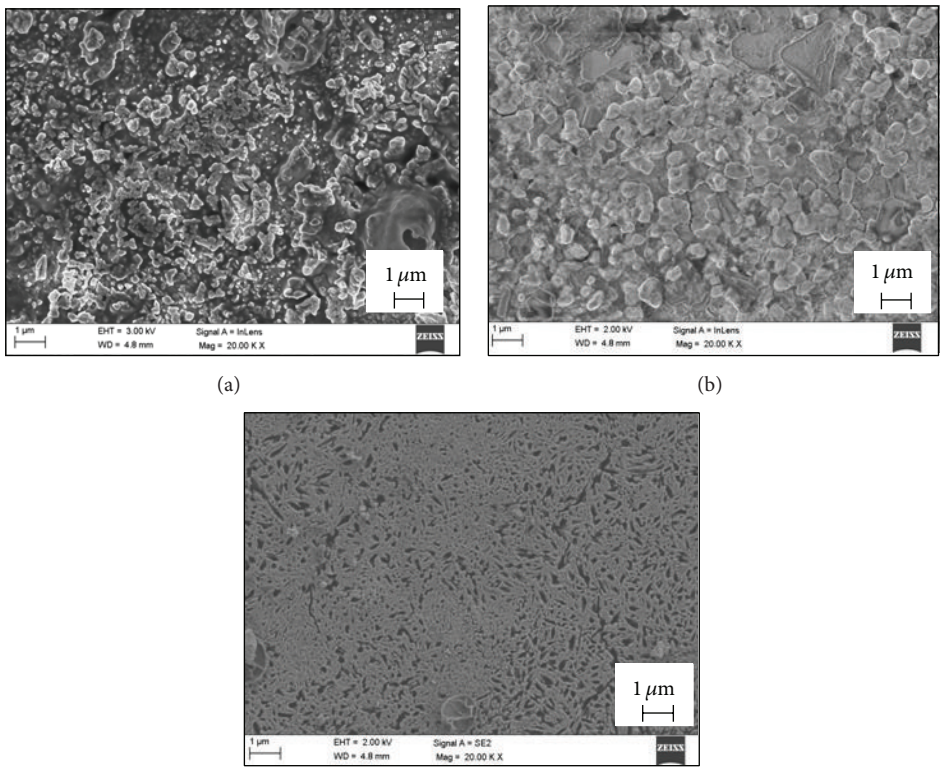


(a) (b)

(c)

Figure 7: SEM of undoped and Cu doped ZnO thin films prepared using precursor solution of molarity of 0.15 M. Here (a), (b), and (c) correspond to samples Z2, Z2C1, and Z2C2, respectively.

Table 1: Crystallite size ($t_{DS}$) and orientation parameter ($\gamma$) of all the samples.

| Samples | $t_{DS}$(nm) | Orientation parameter ($\gamma_{(hkl)}$) | | |
|---|---|---|---|---|
| | (002) | (100) | (002) | (101) |
| Z1 | 21 | 0.141 | 0.772 | 0.156 |
| Z1C1 | 12 | 0.170 | 0.433 | 0.271 |
| Z1C2 | 20 | 0.352 | 0.350 | 0.530 |
| Z2 | 10 | 0.127 | 0.340 | 0.258 |
| Z2C1 | 15 | 0.147 | 0.374 | 0.253 |
| Z2C2 | 15 | 0.145 | 0.375 | 0.253 |

Table 2: Optical band gap of Cu doped ZnO thin films.

| Sample | Composition | Optical band gap (eV) |
|---|---|---|
| Z1 | 0.1 M ZnO | 3.28 |
| Z1C1 | 0.1 M ZnO + 1% $CuCl_2$ | 3.19 |
| Z1C2 | 0.1 M ZnO + 2% $CuCl_2$ | 3.20 |
| Z2 | 0.15 M ZnO | 3.20 |
| Z2C1 | 0.15 M ZnO + 1% $CuCl_2$ | 3.18 |
| Z2C2 | 0.15 M ZnO + 2% $CuCl_2$ | 3.22 |

other to form bigger ones (Figure 6(a)). As the dopant Cu is introduced in 1 at.% in ZnO (sample Z1C1) film surface becomes netted with clear appearances of holes (Figure 6(b)) and for further increased doping of 2 at.% the net making needle-like structures become dominant over the holes (Figure 6(c)).

Surface morphology of samples of molarity 0.15 M are shown in Figure 7. Sample Z2 has random structures spread throughout the surface. For sample Z2C1, these random structures convert in irregular shaped grains. A network of small needle-like structures is seen for Z2C2.

*3.4. Gas Sensing.* For a semiconductor gas sensor, where resistance varies with gas concentration, the sensitivity $S$ is defined as percent ratio of the resistance of the sensing film in air ($R_{\text{air}}$) to the resistance in the presence of the gas ($R_{\text{gas}}$) [26] at a particular temperature; that is,

$$S(\%) = \left(\frac{R_{\text{air}}}{R_{\text{gas}}}\right) \times 100. \quad (2)$$

For each concentration of analyte gas, which in the present case is $CO_2$, the temperature of the films is varied from 200 to 450°C in steps of 50°C and observations are taken. Before introducing the gas, sensing film is allowed to stabilize to ensure fixed initial reading for gas sensing application [27].

Figures 8 and 9 show the effect of temperature on the sensitivity of undoped and copper doped ZnO thin films for four different carbon dioxide concentrations.

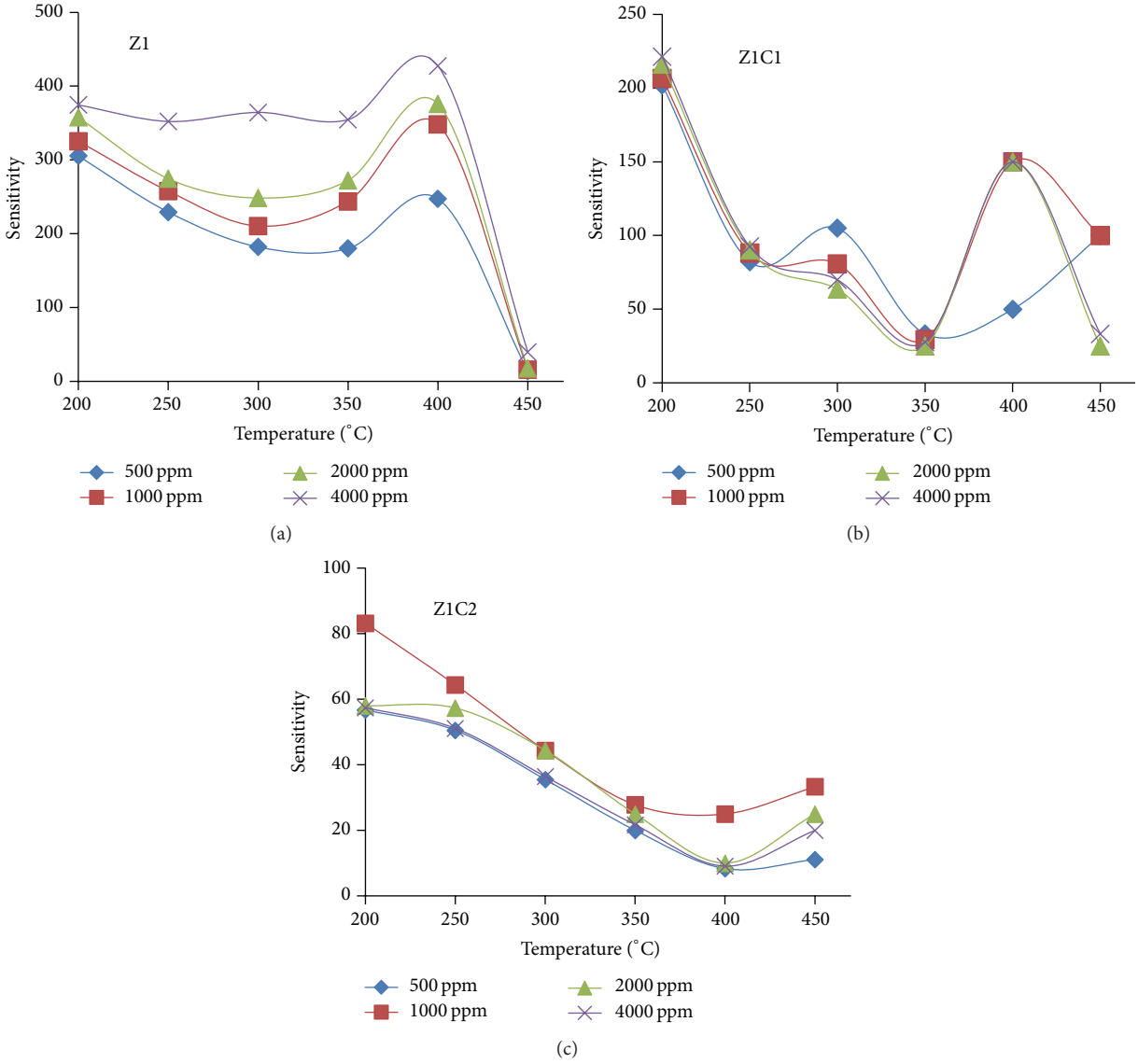


FIGURE 8: Variation of sensitivity of undoped and Cu doped ZnO thin film samples at various $CO_2$ concentrations with temperature. Here (a), (b), and (c) correspond to samples Z1, Z1C1, and Z1C2, respectively, prepared using precursor solution of molarity of 0.1 M.

For sample Z1, sensitivity is maximum at 400°C for all concentrations of $CO_2$ and the sensitivity increases with increase in concentration of $CO_2$. For sample Z1C1, the sensitivity is again maximum at 400°C except for 500 ppm concentration whereas for sample Z1C2 the sensitivity is minimum at 400°C and maximum at 200°C. Such behavior can be attributed to the changing surface morphology of samples (Figure 8).

For sample Z2, maximum sensitivity occurs below 300°C whereas for sample Z2C1 maxima occur at 300°C. For sample Z2C2, again the sensitivity is maximum at lower temperature. It is seen that presence of more and more dopant decreases the sensitivity of the films towards carbon dioxide.

The variation in sensitivity with temperature for 500, 1000, 2000, and 4000 ppm of $CO_2$ concentration is shown in Figures 10(a), 10(b), 10(c) and 10(d) respectively.

The sensitivity has high value at 200°C for samples Z1C1 and Z1C2 at all gas concentrations. However, sample Z1C2 has maximum sensitivity for 1000 ppm at 200°C. An increase in temperature decreases the sensitivity in both these samples whereas for samples Z2C1 and Z2C2 the sensitivity has low value at low operating temperature. Sample Z2C1 has maximum sensitivity at 300°C for 500 ppm. Sample Z2C2 has maximum sensitivity at 250°C for 2000 ppm.

Band theory as applied to gas sensors has been the subject of intense study for a number of years [28, 29]. The analyte carbon dioxide gas interacts with the surface of the metal oxide film (generally through surface adsorbed oxygen ions), which results in a change in charge carrier concentration [30] altering the conductivity (or resistivity) of the material. An n-type semiconductor is one where the majority charge carriers are electrons, and upon interaction with a reducing gas an

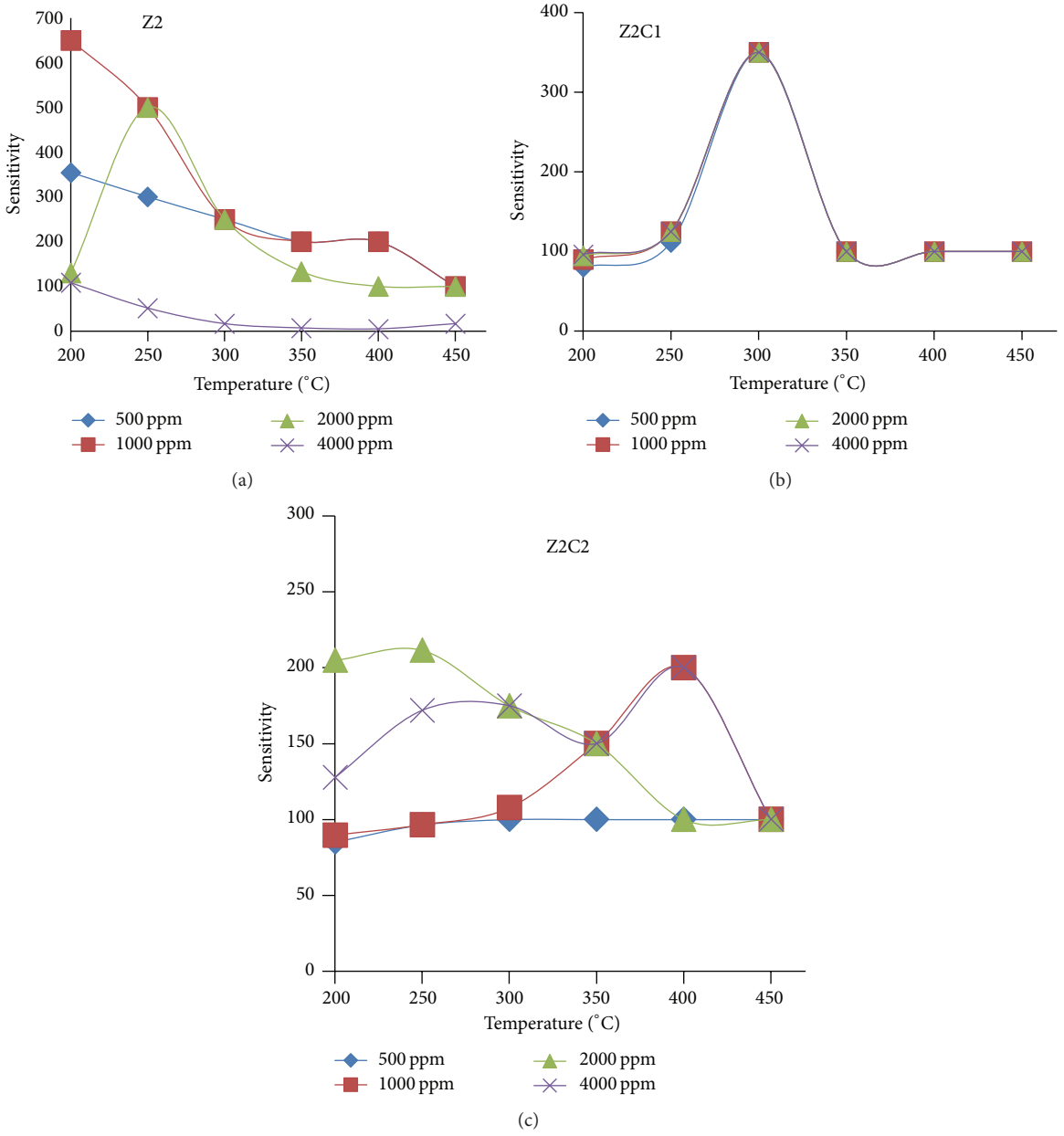


FIGURE 9: Variation of sensitivity of undoped and Cu doped ZnO thin film samples at various $CO_2$ concentrations with temperature. Here (a), (b), and (c) correspond to samples Z2, Z2C1, and Z2C2, respectively, prepared using precursor solution of molarity 0.15 M.

increase in conductivity occurs. However, change in charge carrier concentration in the sample also depends upon the amount of the adsorbed gas which in turn depends on the surface morphology. Thus, the nature of the analyte gas and the surface morphology of the films both should be taken into account while comparing the resistance, $R_{gas}$, of a sample in presence of varying concentration of the gas.

## 4. Conclusions

Nanocrystalline Cu doped ZnO films have been successfully deposited on glass substrates by spray pyrolysis and their structural and optical properties have been investigated. The crystallite size decreases with increase in molarity of precursor solution whereas with doping the crystallite size increases in general. Doping increases the transmittance of the films whereas optical band gap first decreases and then increases as the dopant concentration is gradually increased for both molarities in reference. As the doping increases, the SEM shows formation of irregular shaped grains and then netted structure with holes followed by net making needle-like structures becoming dominant over the holes for both molarities. Response of these films for carbon dioxide has been studied. Undoped ZnO shows maximum sensitivity at 400°C for higher concentration of $CO_2$. The sensitivity of Cu doped sample is

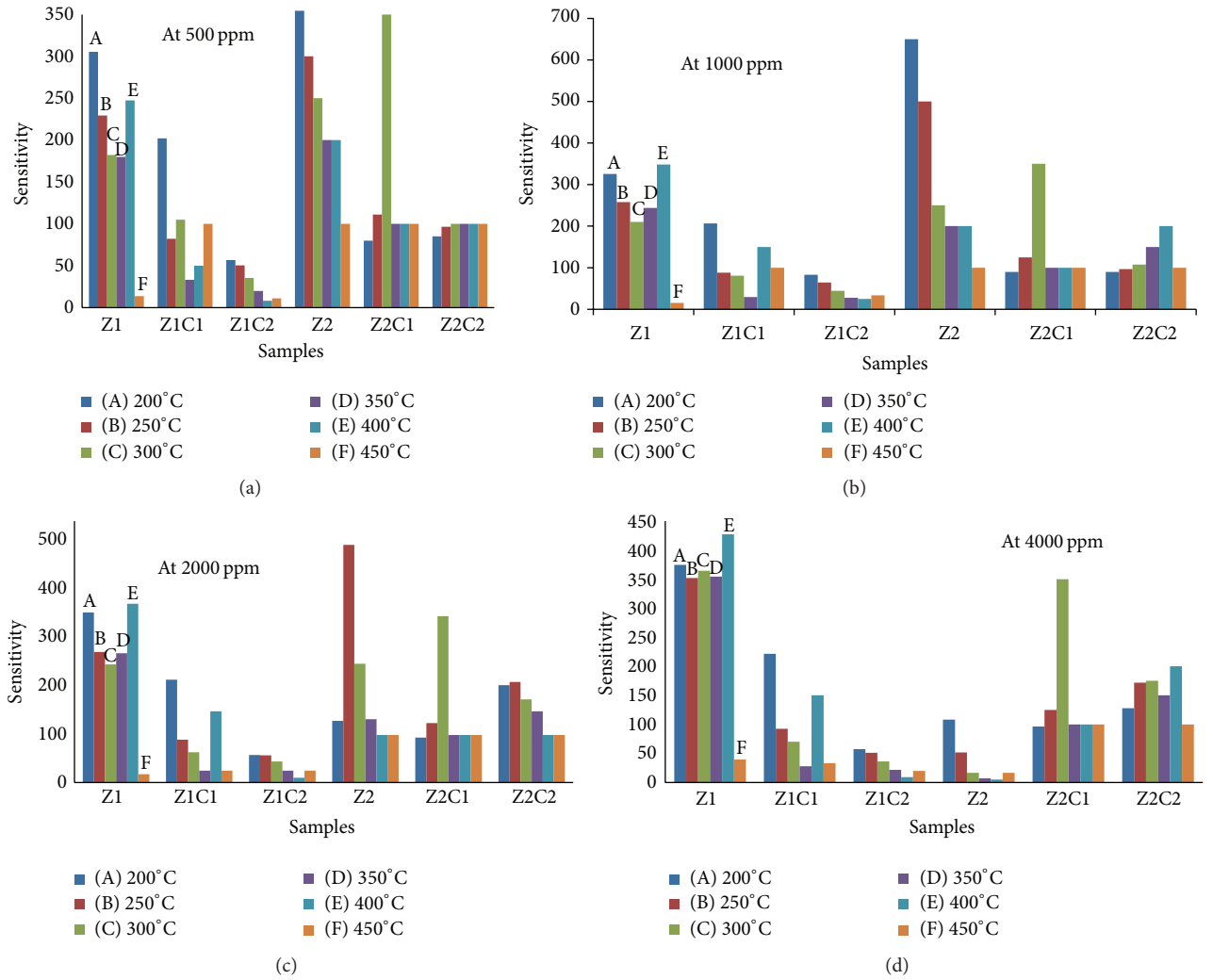


FIGURE 10: (a) Variation of sensitivity of undoped and Cu doped ZnO thin film samples at 500 ppm $CO_2$ concentration with temperature. (b) Variation of sensitivity of undoped and Cu doped ZnO thin films sample at 1000 ppm $CO_2$ concentrations with temperature. (c) Variation of sensitivity of undoped and Cu doped ZnO thin films sample at 2000 ppm $CO_2$ concentrations with temperature. (d) Variation of sensitivity of undoped and Cu doped ZnO thin film samples at 4000 ppm $CO_2$ concentration with temperature.

maximum at 200°C for all $CO_2$ concentrations from 500 to 4000 ppm.

## Conflict of Interests

The authors declare that there is no conflict of interests regarding the publication of this paper.

## References

[1] A. K. Das, P. Misra, and L. M. Kukreja, "Effect of Si doping on electrical and optical properties of ZnO thin films grown by sequential pulsed laser deposition," *Journal of Physics D: Applied Physics*, vol. 42, no. 16, Article ID 165405, 2009.

[2] S. Y. Pung, C. S. Ong, K. Mohd Isha, and M. H. Othman, "Synthesis and characterization of Cu-doped zno nanorods," *Sains Malaysiana*, vol. 43, no. 2, pp. 273–281, 2014.

[3] B. Allabergenov, O. Tursunkulov, A. I. Abidov, B. Choi, J. S. Wook, and S. Kim, "Microstructural analysis and optical characteristics of Cu-doped ZnO thin films prepared by DC magnetron sputtering," *Journal of Crystal Growth*, vol. 401, pp. 573–576, 2014.

[4] Y.-Q. Bie, Z.-M. Liao, P.-W. Wang et al., "Single ZnO nanowire/p-type GaN heterojunctions for photovoltaic devices and UV light-emitting diodes," *Advanced Materials*, vol. 22, no. 38, pp. 4284–4287, 2010.

[5] P. S. Shewale, V. B. Patil, S. W. Shin, J. H. Kim, and M. D. Uplane, "$H_2S$ gas sensing properties of nanocrystalline Cu-doped ZnO thin films prepared by advanced spray pyrolysis," *Sensors and Actuators B: Chemical*, vol. 186, pp. 226–234, 2013.

[6] A. T. Marin, D. Muñoz-Rojas, D. C. Iza, T. Gershon, K. P. Musselman, and J. L. MacManus-Driscoll, "Novel atmospheric growth technique to improve both light absorption and charge collection in ZnO/$Cu_2O$ thin film solar cells," *Advanced Functional Materials*, vol. 23, no. 27, pp. 3413–3419, 2013.

[7] J.-H. Jeon, S.-Y. Jeong, C.-R. Cho et al., "Heteroepitaxial relation and optical properties of Cu-doped ZnO films grown by using pulsed laser deposition," *Journal of the Korean Physical Society*, vol. 54, no. 2, pp. 858–862, 2009.

[8] M. Bedir, M. Öztas, A. N. Yazici, and E. V. Kafadar, "Characterization of undoped and Cu-doped ZnO thin films deposited on glass substrates by spray pyrolysis," *Chinese Physics Letters*, vol. 23, no. 4, pp. 939–942, 2006.

[9] M. B. Rahmani, S. H. Keshmiri, M. Shafiei et al., "Transition from n- to p-type of spray pyrolysis deposited Cu doped ZnO thin films for $NO_2$ sensing," *Sensor Letters*, vol. 7, no. 4, pp. 621–628, 2009.

[10] S. Dixit, A. Srivastava, A. Srivastava, and R. K. Shukla, "Effect of toxic gases on humidity sensing property of nanocrystalline ZnO film," *Journal of Applied Physics*, vol. 102, no. 11, Article ID 113114, 2007.

[11] B. Allabergenov, S.-H. Chung, S. M. Jeong, S. Kim, and B. Choi, "Enhanced blue photoluminescence realized by copper diffusion doping of ZnO thin films," *Optical Materials Express*, vol. 3, no. 10, pp. 1733–1741, 2013.

[12] K. P. Misra, R. K. Shukla, A. Srivastava, and A. Srivastava, "Blueshift in optical band gap in nanocrystalline $Zn_{1-x}Ca_xO$ films deposited by sol-gel method," *Applied Physics Letters*, vol. 95, no. 3, Article ID 031901, 2009.

[13] C.-H. Hsu, L.-C. Chen, and X. Zhang, "Effect of the CU source on optical properties of CuZnO films deposited by ultrasonic spraying," *Materials*, vol. 7, no. 2, pp. 1261–1270, 2014.

[14] C. Wang, Z. Chen, Y. He, L. Li, and D. Zhang, "Structure, morphology and properties of Fe-doped ZnO films prepared by facing-target magnetron sputtering system," *Applied Surface Science*, vol. 255, no. 15, pp. 6881–6887, 2009.

[15] V. S. Kalyamwar, F. C. Raghuwanshi, N. L. Jadhao, and A. J. Gadewar, "Zinc oxide nanostructure thick films as $H_2S$ gas sensors at room temperature," *Journal of Sensor Technology*, vol. 3, no. 3, pp. 31–35, 2013.

[16] F. K. Shan, B. I. Kim, G. X. Liu et al., "Blue shift of near band edge emission in Mg doped ZnO thin films and aging," *Journal of Applied Physics*, vol. 95, no. 9, pp. 4772–4776, 2004.

[17] D. Mishra, A. Srivastava, A. Srivastava, and R. K. Shukla, "Bead structured nanocrystalline ZnO thin films: synthesis and LPG sensing properties," *Applied Surface Science*, vol. 255, no. 5, pp. 2947–2950, 2008.

[18] G. Shanmuganathan and I. B. Shameem Banu, "Influence of codoping on the optical properties of ZnO thin films synthesized on glass substrate by chemical bath deposition method," *Advances in Condensed Matter Physics*, vol. 2014, Article ID 761960, 9 pages, 2014.

[19] P. S. Patil, "Versatility of chemical spray pyrolysis technique," *Materials Chemistry and Physics*, vol. 59, no. 3, pp. 185–198, 1999.

[20] P. Samarasekara, N. U. S. Yapa, N. T. R. N. Kumara, and M. V. K. Perera, "$CO_2$ gas sensitivity of sputtered zinc oxide thin films," *Bulletin of Materials Science*, vol. 30, no. 2, pp. 113–116, 2007.

[21] T. M. Hammad, J. K. Salem, R. G. Harrison, R. Hempelmann, and N. K. Hejazy, "Optical and magnetic properties of Cu-doped ZnO nanoparticles," *Journal of Materials Science: Materials in Electronics*, vol. 24, no. 8, pp. 2846–2852, 2013.

[22] G.-H. Zhang, X.-Y. Deng, H. Xue, and G. Xiang, "Engineering of electronic and optical properties of ZnO thin films via Cu doping," *Chinese Physics B*, vol. 22, no. 4, Article ID 047803, 2013.

[23] A. Srivastava, N. Kumar, K. P. Misra, and S. Khare, "Blue-light luminescence enhancement and increased band gap from calcium-doped zinc oxide nanoparticle films," *Materials Science in Semiconductor Processing*, vol. 26, no. 1, pp. 259–266, 2014.

[24] A. Ashour, M. A. Kaid, N. Z. El-Sayed, and A. A. Ibrahim, "Physical properties of ZnO thin films deposited by spray pyrolysis technique," *Applied Surface Science*, vol. 252, no. 22, pp. 7844–7848, 2006.

[25] J. P. Upadhyay, S. R. Vishwakarma, and H. C. Prasad, "Studies of electrical and optical properties of $SnO_2$:P films," *Thin Solid Films*, vol. 169, no. 2, pp. 195–204, 1989.

[26] R. S. Khadayate, R. B. Waghulde, M. G. Wankhede, J. V. Sali, and P. P. Patil, "Ethanol vapour sensing properties of screen printed $WO_3$ thick films," *Bulletin of Materials Science*, vol. 30, no. 2, pp. 129–133, 2007.

[27] P. Mitra, A. P. Chatterjee, and H. S. Maiti, "ZnO thin film sensor," *Materials Letters*, vol. 35, no. 1-2, pp. 33–38, 1998.

[28] N. Yamazoe, J. Fuchigami, M. O. Kishikawa, and T. Seiyama, "Interactions of tin oxide surface with $O_2$, $H_2O$ and $H_2$," *Surface Science*, vol. 86, pp. 335–344, 1979.

[29] N. Barsan, M. Schweizer-Berberich, and W. Göpel, "Fundamental and practical aspects in the design of nanoscaled SnO2 gas sensors: a status report," *Fresenius' Journal of Analytical Chemistry*, vol. 365, no. 4, pp. 287–304, 1999.

[30] N. Bârsan and U. Weimar, "Understanding the fundamental principles of metal oxide based gas sensors; the example of CO sensing with $SnO_2$ sensors in the presence of humidity," *Journal of Physics: Condensed Matter*, vol. 15, no. 20, pp. R813–R839, 2003.

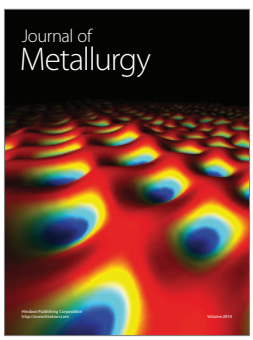

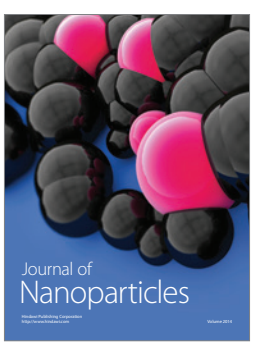

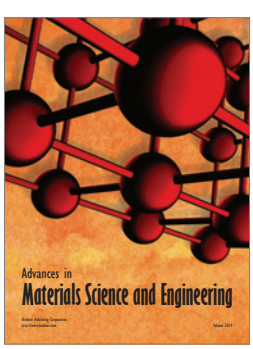

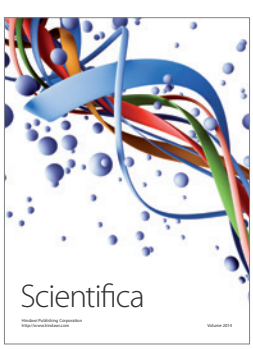

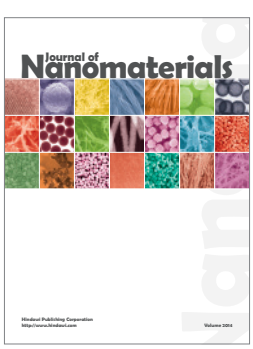

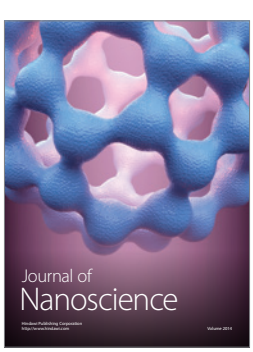

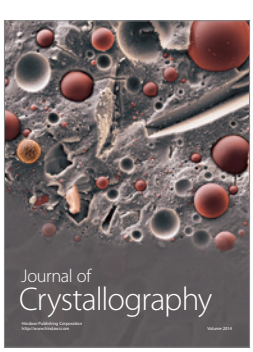

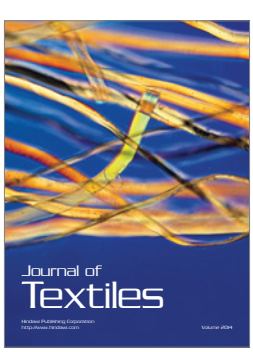


Hindawi

Submit your manuscripts at
http://www.hindawi.com